FRONTAL THORACIC RESPONSE TO DYNAMIC LOADING: THE ROLE OF SUPERFICIAL TISSUES, VISCERA, AND THE RIB CAGE

Richard Kent, University of Virginia
Daisuke Murakami and Seiichi Kobayashi, Nissan Motor Company, Ltd.

ABSTRACT

Three post-mortem human subjects were subjected to dynamic, non-injurious (nominal 20% chest deflection), anterior thoracic loading using a hub, a single diagonal belt, X-type double diagonal belts, and a distributed load. The test matrix also included three thoracic tissue conditions. First, the thoraces were tested intact. Second, they were tested in a "denuded" condition. For this condition, all tissue superficial to the rib cage (skin, fat, muscle) was removed. Finally, the thoraces were tested in an "eviscerated" condition. For this condition, the internal viscera (organs, vasculature, visceral fat, etc.) was removed. The intact thoraces were found to have significantly greater mean stiffness than the eviscerated or denuded thoraces (paired t-test $p < 0.05$). The intact distributed (598.7 N/cm) and double-diagonal belt (529.2 N/cm) conditions were the stiffest, followed by the single diagonal belt (383.5 N/cm) then the hub (170.0 N/cm). The degree to which the soft tissues influenced the response depended on the loading condition. For the hub and distributed loading conditions, the denuded thoraces were approximately 60% of the stiffness of the intact thoraces and the eviscerated thoraces were approximately 30%. The diagonal belt and X-type double diagonal belt loading conditions were not as sensitive to tissue condition. For those loading conditions, the denuded thoraces were approximately 85% of the intact stiffness and the eviscerated thoraces were approximately 55%. The findings of this study indicate the importance of the shoulder in the overall thoracic stiffness. The two loading conditions that did not engage the shoulder (hub, distributed) were highly sensitive to the presence of the soft tissues of the thorax. In contrast, the two loading conditions that engage the shoulder were less sensitive to the removal of the soft tissues. This study provides important validation data for thoracic models since the role of the bones, the organs, and the superficial flesh has been quantified for multiple loading conditions.

Keywords: Thorax, finite element modeling, validation data, restraint systems, thoracic injury

ANALYTICAL AND COMPUTATIONAL MODELS play an important role in the design of vehicular occupant protection systems. In particular, thoracic models have been used extensively to study restraint performance and injury risk. One of the earliest models used to predict thoracic response to impact was developed by Lobdell, *et al*. (1973). They proposed an arrangement of masses, springs, and dashpots to simulate the force-deformation response measured by Kroell, *et al*. (1971, 1974) using blunt hub impacts to the chests of post-mortem human subjects (PMHS). The various lumped parameters were described as representing the contributions of the bony and visceral structures in the thorax, but this apportionment was not explicitly supported by the experimental data. This model has been used extensively in the literature, and current occupant protection systems (door padding crush response in a side impact, for example) and analysis methodologies are designed based on research done with this model (Viano *et al.*, 1987a, b, Crandall *et al.* 2000, Kent *et al.* 2004, Shaw *et al.* 2005). In 1988, Deng proposed a two-dimensional alternative to the one-dimensional Lobdell model. Unlike the Lobdell model, which was developed based on pendulum impact tests, the Deng model was developed using data from vehicle crash tests of intact PMHS and involved both frontal and lateral validation, though restraint loading was not considered. King *et al.* (1991) proposed a more elaborate lumped parameter model based on 17 PMHS side impacts into stationary walls. This one-dimensional model is arranged to have five degrees of freedom, with masses representing the shoulder, rib cage, abdominal casing, and pelvis. Elements are used to represent the tissue separating each of these elements of the thorax. Again, there is no experimental validation of the apportionment of responses in this manner.

As computational power has increased, so have the complexity and applicability of thorax models. Multi-body models, especially within the MADYMO software package, have become industry standard tools, and thoracic finite element (FE) models have been in use for over a decade.

One of the earliest FE models of the complete human thorax was developed by Stokes and Laible (1990) to investigate how asymmetric growth of the thorax may contribute to scoliosis. This model consisted only of a simplified rib cage and intercostal ligaments and was not validated for impacts. Perhaps the first model intended to study traumatic thoracic injury was developed by the U.S. National Highway Traffic Safety Administration (Plank, *et al.*, 1989, 1994, 1998). The model consists of twelve thoracic and five lumbar spinal vertebrae and the associated intervertebral disks; twelve ribs; back, abdominal, and intercostal muscles; and a homogeneous representation of the viscera. Material properties from the literature were used including homogeneous, isotropic, linear elastic properties for the bone, cartilage, and ligaments and incompressible viscoelastic properties for the entire interior thoracic volume and some of the muscle elements. These properties were optimized so that the gross overall frontal impact response of the thorax fit reasonably well within a prescribed corridor based on impact tests of the thoraces of intact PMHS (Kroell *et al.* 1971, 1974).

Lizee *et al.* (1998) reported on a 50th percentile male full-body human model developed jointly by four European laboratories: CEESAR, LAB/PSA, ENSAM, and INRETS. Existing material properties from the literature were used and optimized based on PMHS and human volunteer tests, including crash tests, impactor tests, and belt compression tests over a range of impact energies and directions. The soft tissues filling the rib cage, abdomen, and pelvis were represented globally as three uniform meshes (representing the lungs and heart, the spleen and stomach, and the intestines, respectively) comprised of viscoelastic brick elements. Individual organs and tissues within the thorax were not modeled due to a lack of mechanical information. Muscles and adipose tissue covering the rib cage and abdominal contents were represented by a single layer of linear viscoelastic brick elements, and the skin was represented by a second layer of linear viscoelastic brick elements. Wang and Yang (1998) published a model that was similar to the Lizee model except available anthropometric data were used to construct a detailed model of the heart and aorta, including the structure around the aortic arch. Deng *et al.* (1999) presented a model based on digital surface images of a human skeleton, heart, lungs, and major blood vessels. Material properties were based on the literature, with the ribs modeled as homogeneous linear elastic material, thoracic vertebrae modeled as rigid bodies, the muscles and diaphragm modeled as linear elastic membranes, and the heart and lungs modeled as hyperelastic materials. Again, the primary structural validation standards for these models were based on the data from hub impact tests of intact PMHS.

More advanced thoracic finite element models are currently under development, as reported by Huag *et al*. (1999), Ruan *et al.* (2003), Iwamoto *et al.* (2000), Petit *et al.* (2003), Murakami *et al.* (2004) and others. Contemporary models include more detailed geometric and material descriptions of bones and cartilage structures, intercostals and abdominal muscles, large blood vessels, heart, esophagus, diaphragm, lungs, and superficial tissues. They are also modular, to accommodate refined submodels of individual organs or tissue as the necessary data become available.

The refinement and optimization of these human body finite element models is critical for the efficient development of advanced occupant protection strategies, and is a central goal of the injury biomechanics community. As described above, however, any model development effort is limited by the lack of experimental input and validation data. Missing information includes detailed and appropriate constitutive models of biological tissues, as well as appropriate macroscopic (structural) validation response information. In particular, nearly all of the structural validation data available for the thorax were generated using a hub impact methodology and an intact thorax. As such it is not possible to apportion the overall structural response among the various components of the thorax (e.g., superficial tissues, internal viscera, bones). The objective of this study was therefore to develop a novel set of validation guidelines for the anteriorly loaded thorax by apportioning the contributions of the various thoracic components to the overall response and to use a diverse set of loading conditions - not just a hub. Specifically, the goal of this study was to quantify the contributions of the superficial tissues, the internal viscera, and the bony rib cage to the force-deflection response of the thorax when loaded anteriorly by a hub, a diagonal belt, a distributed load, and two diagonal belts crossed over the chest. This is an extension of our earlier work, which focused on these four loading conditions with an intact thorax (Kent *et al.* 2003, 2004). In that earlier work, we described how impact hub tests are inadequate for robust structural validation for two primary reasons. First, inertial contributions dominate the force generated by the struck thorax, which is not representative of restraint loading where the elastic and viscous characteristics dominate the response of the deforming thorax. Second,

restraint loading involves anatomical structures that are not loaded by a hub. Our previous work has shown that the shoulder, clavicle, and superior ribs contribute substantially to the overall structural thoracic response to loading. Building upon the pioneering blunt hub impact data historically used for model validation, this work attempts to provide a complimentary and more appropriate set of structural validation standards for computational models intended to be used for restraint design.

METHODS

Three PMHS were subjected to non-injurious (nominal 20% chest deflection) anterior thoracic loading (Table 1). A factorial experimental design was used. The factors were the loading condition (4 levels) and the tissue condition (3 levels). The four loading conditions were a hub, a diagonal belt, an X-type double diagonal belt, and a distributed load. The three tissue conditions were intact, denuded, and eviscerated (Table 2).

Table 1 – Description of Test Subjects

PMHS I.D.	Age/ Gender	Mass (kg)	Stature (cm)	BMI[¥] (kg/m^2)	Chest depth (mm) (4^{th} rib/8^{th} rib)*	Chest breadth (mm) (4^{th} rib/8^{th} rib)*	Cause of death†	Bone density [§]
155	71/F	54.4	166	19.7	229/ 210	350/ 295	MI	NA
173	67/F	57.2	162	21.8	155/ 160	280/ 270	CVA	273.2
178	73/M	80.7	182	24.4	230/ 225	360/ 360	NA	229.7
mean	70.3	64.1	170	22.0	204.7/198.3	330.0/308.3		251.5

*Supine, unpressurized. †MI – Myocardial infarction, CVA – Cerebrovascular accident (multiple thromboembolic strokes). [§]Houndsfield units from calibrated CT scan of lumbar vertebra (NA – Not Available). [¥]BMI - Body Mass Index (stature over weight squared).

The loading apparatus and the preconditioning/randomization test strategy described in detail in our earlier studies (Kent *et al.* 2003, 2004) (Figure 1) were used for these tests. This system is a refinement of one originally described by Cesari and Bouquet (1990). A hydraulic master-slave cylinder arrangement with a high-speed material testing machine (Instron model 8874, Canton, Massachusetts) was used to generate chest deflection at a rate similar to that experienced by restrained PMHS in 48 km/h frontal sled tests (see Kent *et al*. 2004 for more description of this target rate and how it was developed). Diagonal belt and distributed loading were performed via cable-belt systems passing over the thoraces of PMHS positioned supine on a table. The posterior boundary condition was a rigid flat plate on which the subject was laid. The subject was not fixed to the flat plate and the spinal curvature was not controlled other than by the flat plate interface. The thoracic spine was virtually free of lordotic or kyphotic curvature at the start and throughout each test. All belts were constructed of spectra fiber-reinforced sail cloth, which conforms to the chest similarly to a seatbelt, but did not elongate measurably during loading. This material was chosen rather than actual seatbelt webbing (which would stretch nominally 2%-4% in these tests) so that the measured force-deflection response would be a characteristic of the thorax rather than of the thorax in series with a deforming element. While the thoracic interaction with the belt might be affected slightly had the belt been permitted to stretch, it was decided that the use of the sail cloth was a desirable tradeoff between reasonable thoracic loading and the ability to isolate the thoracic response. The use of this material will also presumably facilitate computational modeling of the test setup since the strain of the belt material in these tests is virtually zero.

The 5-cm-wide diagonal belt passed over the shoulder and crossed the anterior thorax approximately 30° from the sagittal plane. The belt engaged the PMHS clavicle at approximately the proximal third, crossed the midline approximately mid-sternally, and exited the body laterally at approximately the superior-inferior location of the 9th rib. The double diagonal belt condition involved a second diagonal belt oriented symmetrically to the first diagonal belt. For distributed loading, a 20.3-cm-wide belt loaded the area approximately between the second and seventh ribs. The hub load was applied with a 15.2-cm diameter steel circular plate intended to mimic the loading surface described by Kroell *et al*. (1971, 1974). The center of the hub was located at the intersection of the mid-sagittal plane and approximately the 4^{th} intercostal space. A frame with a bearing track was used with the hub condition to ensure anterior-posterior loading and to prevent the hub from rotating during loading.

Table 2 – Test Matrix

Loading Condition	Tissue Condition	Subject I.D.	Test No.
Hub	Intact	155	CADVE 67
		173	CADVE 103
		178	CADVE 127
	Denuded	155	CADVE 76
		173	CADVE 112
		178	CADVE 129
	Eviscerated	155	CADVE 83
		173	CADVE 114
		178	CADVE 135
Single Diagonal Belt*	Intact	173	CADVE 105
		178	CADVE 124
	Denuded	173	CADVE 110
		178	CADVE 131
	Eviscerated	173	CADVE 115
		178	CADVE 137
Double Diagonal Belts	Intact	155	CADVE 71
		173	CADVE 107
		178	CADVE 122
	Denuded	155	CADVE 78
		173	CADVE 109
		178	CADVE 132
	Eviscerated	155	CADVE 81
		173	CADVE 116
		178	CADVE 136
Distributed*	Intact	173	CADVE 100
		178	CADVE 120
	Denuded	173	CADVE 111
		178	CADVE 133
	Eviscerated	173	CADVE 117
		178	CADVE 134

*Testing was unsuccessful with these two conditions on the first subject (155). The belts slipped superiorly when load was applied due to decreased thoracic friction when the skin was removed. In subsequent subjects, high-friction flexible sand-paper tape was applied to the posterior surface of the belts, which maintained them in position.

The belt geometry used in these tests was based on belt angles measured at the point of maximum chest deflection (also approximately the point of maximum forward excursion) during a sled test using a 56-km/h NCAP pulse and a research-version combined 3-point + 2-point belt system (Bostrom and Haland 2003). This belt geometry was also similar to that at maximum forward excursion using a production, standard belt with an air bag in a 48 km/h sled test (Kent *et al*. 2001).

Chest deflection was measured anteriorly via string potentiometers attached to the belts or to the hub. For the hub condition, deflection was measured at a single point. For all other conditions, deflection was measured at three points (upper left, middle, lower right). In this paper, the mid-sternal chest deflection is used to define the force-deflection response corridors. The location of this measurement is given by Y_{notch}, defined as the distance from the sternal notch inferiorly along the mid-sternum to the location of the mid-sternal chest deflection measurement site. This distance was constant for all loading conditions on each subject, but varied across PMHS depending on individual anthropometry. In all cases, Y_{notch} was not targeted for reproduction among subjects, but was determined after placing the diagonal belt in a "normal" orientation on the chest. The values of Y_{notch} for subjects 155, 173, and 178 were 10.3 cm, 7.4 cm, and 6.5 cm.

Pre-test CT scans were used to confirm the absence of pre-existing fractures, lesions or other bone pathology in the thoracic cage of the test subjects. Diagnosing rib fractures in a post-mortem subject is difficult (Crandall *et al*. 2000), however, and it is possible that some fractures (such as those resulting from resuscitation efforts) may have existed prior to starting the test program. All subjects were preserved either by freezing or by refrigeration (Crandall 1994), but were allowed to reach room temperature at the core prior to testing, and all subjects were tested at room temperature (22°C ± 3°C). To facilitate handling, the subjects' lower extremities were amputated at the femur mid-shaft. The PMHS were obtained and treated in accordance with the ethical guidelines approved by the Human Usage Review Panel, U.S. National Highway Traffic Safety Administration, Department of Transportation, and all PMHS testing and handling procedures were approved by the University of Virginia (UVA) institutional review board.

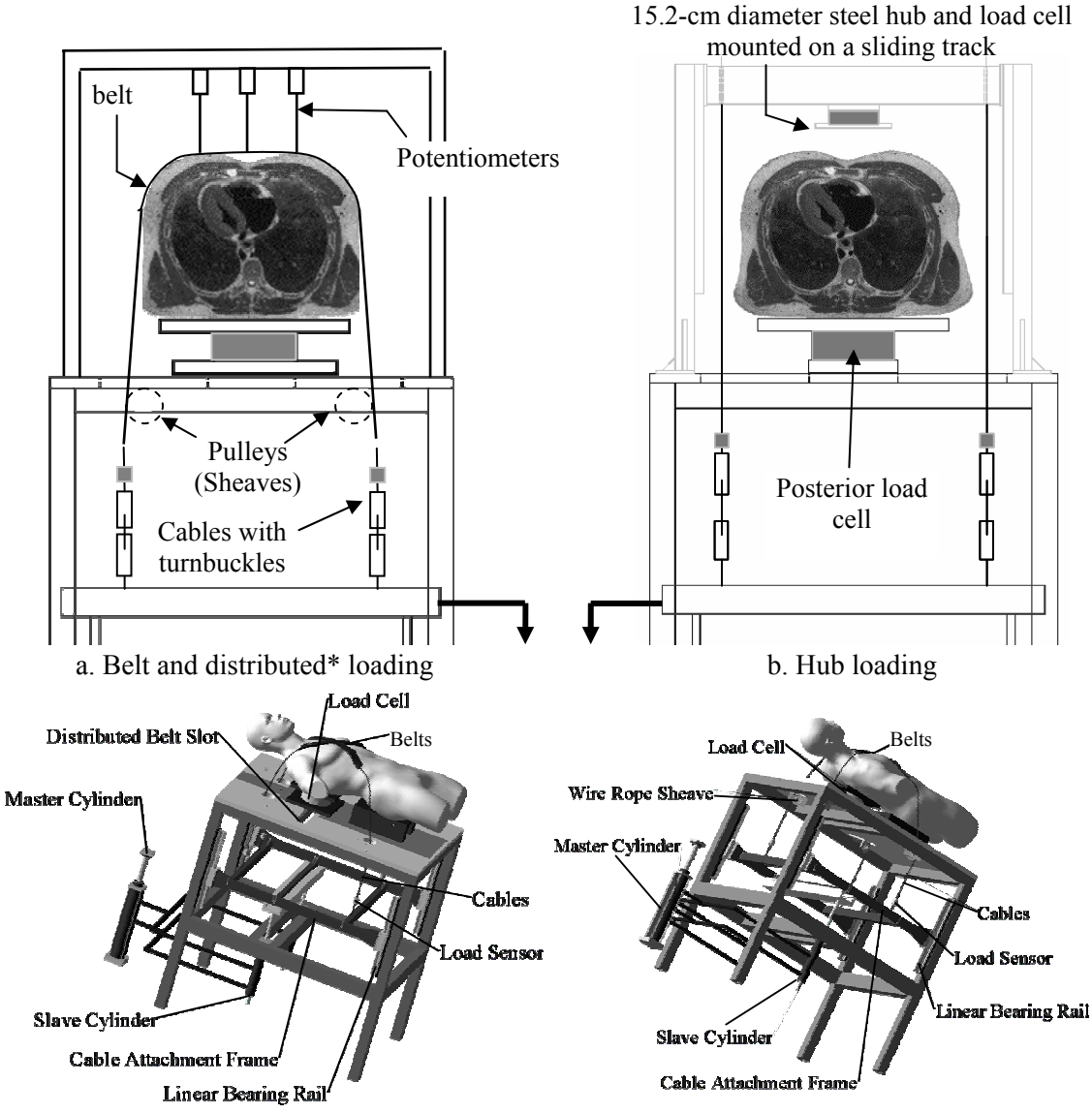

*Distributed belt cables did not pass over pulleys. They went through slots in the table and around a spacer (see Appendix A of Kent *et al*. 2004).

Figure 1. Schematic depictions of test fixture and loading conditions (small triangles represent string potentiometer attachment sites).

To maximize the applicability of the data (i.e., to approach injury levels), but minimize thoracic response changes due to tissue damage, tests were designed to approach, but not exceed, rib fracture threshold for all tests. Since the rib fracture threshold varies widely depending on the subject's age, gender, size, bone condition, and the presence of superficial soft tissues, the applied displacement varied among subjects. The lack of rib fractures was assessed using an acoustic sensor (Nano 30, Physical Acoustics, Princeton Junction, NJ), palpation after each loading cycle, and strain gages mounted on selected ribs. The acoustic sensor, which has an operating range of 125 kHz to 750 kHz, with a center frequency of approximately 140 kHz, was mounted on the superior sternum, immediately inferior to the sternal notch. The signal was amplified 60 dB and low-pass filtered at a cutoff frequency of 400 kHz. Data were sampled at 2.5 MHz using a digital storage oscilloscope. The use of these sensors for crack detection in bone has been discussed in detail by Funk (2000).

First, the thoraces were tested intact. The pulmonary system was pressurized via a tracheostomy to simulate an *in vivo* volume of air in the lungs. Second, the subjects were tested in a "denuded" condition. For this condition, all tissue superficial to the rib cage (skin, fat, muscle) was removed circumferentially around the entire thorax, as was the soft tissue overlaying the shoulder. As shown in Figure 2, the proximal attachment of the biceps brachii was maintained, as was all ligamentus support of the shoulder, clavicle, and scapula. The peritoneal membrane was left intact and the lungs were pressurized for the denuded tests. Finally, the thoraces were tested in an "eviscerated" condition. For this condition, the internal thoracoabdominal viscera (organs, vasculature, visceral fat, etc.) was removed (Figure 2).

Figure 2. Photographs of subject 155 in the intact (left, with hub), denuded (middle), and eviscerated (right) tissue states.

The primary outcome considered in this study was the slope of a linear regression to the cross-plot of the posterior reaction force and the central sternum deflection. This slope is defined as the effective structural stiffness of the thorax. It is important to note that the initial position of the anterior chest changed for the various test conditions. In other words, the initial length of the string potentiometer increased when the superficial tissues were removed and again when the organs were removed. The stiffness was calculated using debiased displacements, so this effect is not contained in the effective stiffness values presented below. The change in initial string length is useful information, however, so plots of force versus both debiased and non-debiased string position are included in the Appendix to illustrate the magnitude of the change in chest depth associated with tissue removal and pulmonary pressurization. The Appendix also illustrates the technique used to determine the stiffness.

RESULTS

As mentioned above, the denuded and eviscerated conditions were not successfully tested on subject 155 using the single diagonal belt and the distributed load. Removal of the skin and other superficial tissues decreased the frictional force between the belt and the anterior chest, so the single

diagonal belt and the distributed belt tended to slide parallel to the surface of the chest when loading was applied. This situation was prevented with subsequent subjects by adhering a high-friction (sand paper) surface to the posterior surface of the belts. The hub condition, which was constrained by the bearing track, and the double-diagonal belt, which was unable to slide due to its inherent geometric stability, did not slide during any tests so those data were collected successfully for all subjects.

Table 3 – Effective Stiffness (Unscaled, All Tests)

Loading Condition	Tissue Condition	PMHS I.D.	Effective Stiffness (N/cm)	Avg.
Hub	Intact	155	184.4	170.0
		173	173.3	
		178	152.3	
	Denuded	155	117.3	99.4
		173	92.2	
		178	88.8	
	Eviscerated	155	94.9	54.1
		173	36.2	
		178	31.2	
Single Diagonal Belt*	Intact	173	386.0	383.5
		178	380.9	
	Denuded	173	295.6	332.5
		178	369.3	
	Eviscerated	173	226.5	264.6
		178	302.6	
Double Diagonal Belts	Intact	155	539.5	529.2
		173	477.7	
		178	570.5	
	Denuded	155	364.1	430.9
		173	391.1	
		178	537.4	
	Eviscerated	155	292.2	272.6
		173	235.7	
		178	289.9	
Distributed*	Intact	173	522.3	598.7
		178	675.0	
	Denuded	173	363.2	362.1
		178	361.0	
	Eviscerated	173	172.4	143.5
		178	114.5	

The intact thoraces were found to have significantly greater mean stiffness than the eviscerated or denuded thoraces (paired t-test $p < 0.05$, Table 3). The distributed (598.7 N/cm) and double-diagonal belt (529.2 N/cm) conditions were the stiffest, followed by the single diagonal belt (383.5 N/cm) then the hub (170.0 N/cm) (Figure 3). Furthermore, the degree to which the soft tissues influenced the response depended on the loading condition (Figure 4). For the hub and distributed loading conditions, the denuded thoraces were approximately 60% of the stiffness of the intact thoraces and the eviscerated thoraces were approximately 30%. The diagonal belt and double diagonal belt loading conditions were not as sensitive to tissue condition. For those loading conditions, the denuded thoraces were approximately 85% of the intact stiffness. For the single diagonal belt loading, the completely eviscerated thorax retained nearly 70% of the stiffness of the intact thorax, indicating that this is a very efficient manner of loading the shoulder and bony thoracic cage. When the second diagonal belt was added, the eviscerated thorax retained about 50% of the intact stiffness.

DISCUSSION

This study provides validation data that should be considered in the development of thoracic models of impact loading since the role of the bones, the organs, and the superficial flesh has been quantified in a dynamic environment. It is important to model these roles accurately since restraint loading is a dynamic phenomenon that exercises the elastic, viscous, and inertial characteristics of the thoracic structure. In order to be useful for assessing various restraint design concepts, a model must reproduce these characteristics.

The findings of this study indicate the importance of the shoulder in the overall thoracic response to loading. The two loading conditions that did not engage the shoulder (hub, distributed) were highly sensitive to the presence of the soft tissues of the thorax. In contrast, the two loading conditions that engaged the shoulder were less sensitive to the removal of the soft tissues. When only the rib cage was loaded (e.g., with the hub or distributed belt), the soft tissues actually provided more than half of the effective stiffness of the thorax, though that ratio is undoubtedly sensitive to loading rate and thus not generalizable beyond the single chest deflection rate (~1 m/s) tested here. This study also revealed the somewhat surprising finding that removing the superficial soft tissues actually decreased the effective structural stiffness of the thorax. It had been expected that removing this soft tissue layer would allow engagement of the bony thorax and internal organs at a lower magnitude deflection and thus generate an effectively stiffer response. This was not the case. One hypothesized mechanism by which the superficial soft tissues increase the thoracic stiffness is their role in coupling

the thorax. We hypothesize that the skin and, to a lesser extent, the superficial fat and muscles, go into tension when the thorax is deformed. This tensile loading generates a force that increases monotonically with chest deflection. Thus, removal of the superficial tissues removes this alternate load path and decreases the structural stiffness relative to an intact thorax. Additional testing would be helpful for evaluating this hypothesized mechanism. In particular, tests with the organs removed, but the superficial tissues retained, would be a useful expansion of the current study.

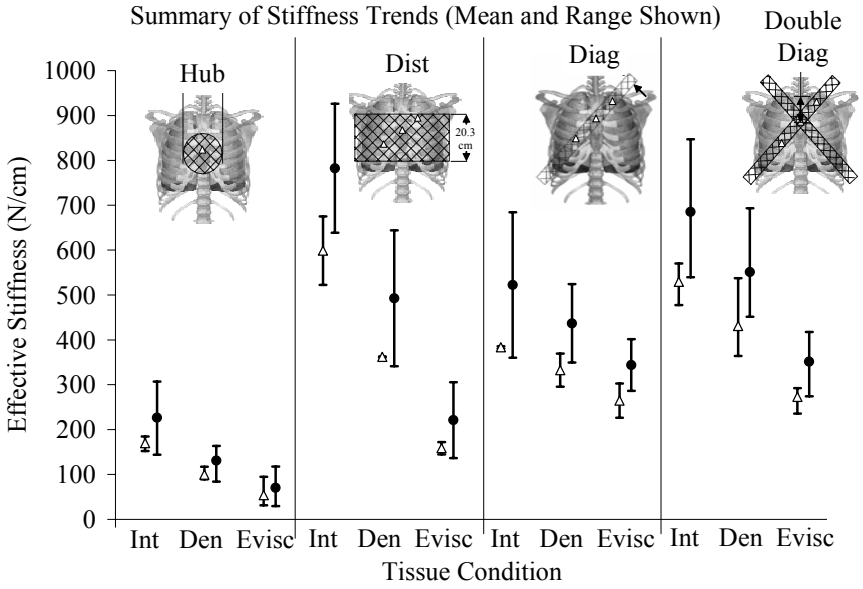

Figure 3. Summary of stiffness trends. The triangles represent the unscaled data. The filled circles represent the data scaled to 50th percentile male using the force and deflection scaling process described by Kent et al. (2004).

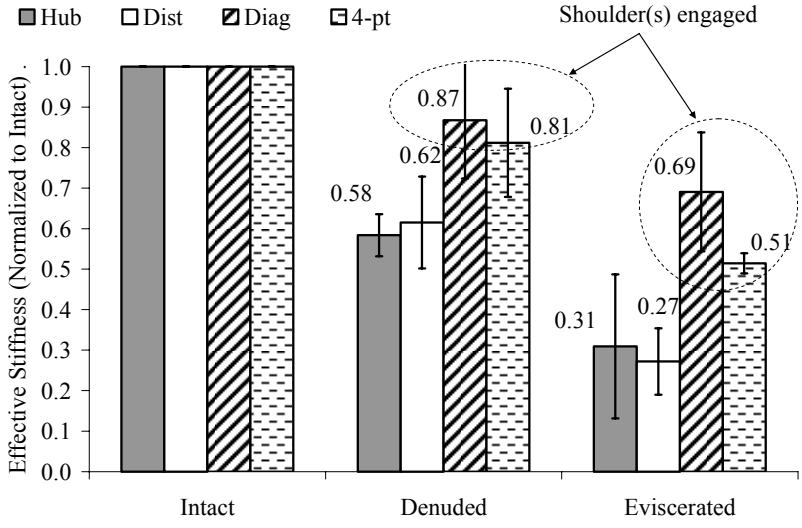

Figure 4. Normalized effective stiffness (unscaled) illustrating the role of shoulder engagement on sensitivity to denuding and eviscerating.

Performing multiple tests on the same thorax was necessary to characterize the response change when the loading condition or tissue state varied since individual variability among subjects is large. This variability would mask the effect of a change in loading condition or tissue state if only a single condition was used on each subject. Despite attempts to avoid injury prior to the final test, there were cases of acoustic emissions consistent with isolated rib fractures prior to the final test and rib fractures were palpable following intact loading. In particular, subject 178 sustained multiple fractures during the course of loading. This was of concern since the rib cage loses stability as ribs progressively fracture and the thoracic stiffness values could potentially be skewed by test order.

Repeated testing was, however, a necessary limitation of this study. Due to the limited number of subjects available for testing, it was not possible to use the data verification scheme employed in our earlier study (Kent *et al*. 2004). The validity of the data from subject 178 was assessed by comparing its trends with the trends from the other two subjects. Compared to the other subjects, the data from subject 178 did overstate slightly the decrease in stiffness that occurred with denuding and eviscerating for all loading conditions, though it showed the same general trends with respect to loading condition and tissue state (Table 3). The role that rib fractures play in the structural response of the dynamically loaded thorax is currently subject to some debate (Yoganandan *et al*. 2004), so this study has not attempted to quantify the effect of pre-existing fractures. Future work should consider this limitation.

This study is considered to be a pilot effort to provide preliminary model validation guidelines. Before formal validation corridors can be developed more tests must be done to improve the robustness of the trends found here. The study is, of course, also limited by the use of PMHS to represent the living human. While muscle tensing is probably not an important factor to consider for this type of loading (Shaw et al. 2005), it is well established that soft tissue autolysis occurs quickly after death. The degree to which this confounds the results of this study is unknown. Other limitations of the PMHS tests presented here include the use of a constrained back condition, which results in a different response than a thorax loaded only by its inertia, as it is in most frontal car crashes. Computed tomography studies performed at the University of Virginia have shown that the posterior ribs do rotate when an anterior load is applied (Ali *et al*. 2005). Therefore, one possible effect of the posterior plate is an increase in stiffness due to constraint of the costovertebral and costotransverse joints. To our knowledge, this increase has never been quantified and is likely small compared to inter-specimen variability, but it is a possible confounder of the trends found here since the stiffness increase may be systematically related to loading condition and tissue state. This loading environment has a strong precedent in the literature, however, and is a reasonable tradeoff between control and applicability to the restraint loading environment.

The use of the posterior reaction force rather than the anteriorly applied force minimizes the inertial contribution to the response. There is an inertial effect in these tests, however, as evidenced by the oscillations that can be seen in the early portion of the force-time signals. This effect is not, however, assumed to be due to the thorax, but rather to inadequate mechanical isolation of the loading table since a visible vibration of the table could be observed when the input displacement was applied to the chest. As a result, we have treated this oscillation as a damped, second-order artifact and assumed that the effective stiffness of the thorax can be quantified by fitting a line through the oscillations.

The corridors presented here are a useful but limited biofidelity assessment tool in that they define the kinetic response of the thorax to four types of loading using a single geometric arrangement for each. In a dynamic collision environment, the thorax-restraint geometry changes throughout the event as the occupant's torso rotates forward. As a result, attempts to validate a thoracic model using these corridors should be accompanied by full-scale sled tests to provide a supporting kinematic biofidelity assessment. Future work should include a sensitivity study to evaluate how changes in belt angles relative to the torso influence the kinetic response and additional tests or analyses to apportion the roles of elastic and viscous thoracic properties.

CONCLUSIONS

This pilot study has provided an initial assessment of the decrease in the structural stiffness of the dynamically loaded thorax that occurs when the superficial soft tissues and the internal viscera are removed. It therefore provides important guidelines for modeling the role of these structures and for understanding how external loads are borne by the deforming thorax. The results show that the decrease in structural stiffness varies by loading condition. The loading conditions that engaged the shoulder(s) exhibited smaller reductions in structural stiffness when the soft tissues were removed. For example, a thorax loaded by a diagonal belt having geometry similar to an automotive shoulder belt retains about 70% of its structural stiffness when completely eviscerated and denuded. Loading conditions that do not engage the shoulder rely much more on the soft tissue for structural support. When loaded by a hub, for example, the eviscerated/denuded thorax retains only about 30% of its intact stiffness.

ACKNOWLEDGEMENTS

This research was supported by funds from Nissan Motor Company, Ltd., though the findings do not necessarily represent the views of this organization. The authors acknowledge the technical input provided by Dr. Yuichi Kitagawa and Dr. Greg Hall during the initial development of this test procedure. Thanks also to the students and staff of the UVA Center for Applied Biomechanics, who assisted in the testing and data reduction

REFERENCES

Ali, T., Kent, R., Murakami, D., Kobayahsi, S. (2005) Tracking rib deformation with increasing chest deflection under load using computed tomography imaging. Paper 2005-01-0299 Society of Automotive Engineers, Warrendale, PA.

Cesari, D. and Bouquet, R. (1990) Behavior of human surrogates under belt loading. Proc. 34th Stapp Car Crash Conference, pp. 73-82.

Crandall J. (1994) The Preservation of Human Surrogates for Biomechanical Studies. PhD Dissertation released by the University of Virginia Department of Mech and Aero Engineering.

Crandall, J, Kent, R, Patrie, J, Fertile, J, Martin, P. (2000) Rib fracture patterns and radiologic detection – a restraint-based comparison. Annual Proceedings/Association for the Advancement of Automotive Medicine; 44:235-59

Crandall, J. R., Cheng, Z, and Pilkey, W.D., (2000) Limiting performance of seat belt systems for the prevention of thoracic injuries. Proc. Instn. Mech. Engrs, **214**, Part D, pp. 127-139.

Deng, Y. C. (1988) Design considerations for occupant protection in side impact - A modeling approach. Proc 32nd Stapp Car Crash Conference, SAE 881713, 1988.

Deng, Y. C., Kong, W. K., and Ho, H. (1999) Development of a finite element human thorax model for impact injury studies. SAE 1999-01-0715.

Funk J (2000) The Effect of Active Muscle Tension on the Axial Impact Tolerance of the Human Foot/Ankle Complex. PhD Dissertation released by the University of Virginia Department of Biomedical Engineering.

Haug, E., Bequgonin, M., Tramecon, A., and Hyncik, L. (1999) Current status of articulated and deformable human models for impact and occupant safety simulation at ESI group. European Conference on Computational Mechanics, Munich, Germany, 1999.

Iwamoto, M., Mike, K., Mohammad, M., Nayef, A., Yang, K.H., Begeman, P.C., King, A.I. (2000) Development of a finite element model of the human shoulder. *Stapp Car Crash Journal,* 44:281-297.

Kent, R., Crandall, J., Bolton, J., Prasad, P., Nusholtz, G., Mertz, H. (2001) The influence of superficial soft tissues and restraint condition on thoracic skeletal injury prediction. Stapp Car Crash Journal 45:183-203.

Kent, R, Sherwood, C, Lessley, D, Overby, B, Matsuoka, F. (2003) Age-related changes in the effective stiffness of the human thorax using four loading conditions. IRCOBI Conference on the Biomechanics of Impact.

Kent, R, Lessley, D, Sherwood, C (2004) Thoracic response corridors for diagonal belt, distributed, four-point belt, and hub loading. Stapp Car Crash Journal 48:495-519.

King, A. I., Huang, Y., and Cananaugh, J. M. (1991) Protection of occupants against side impact. Thirteenth International Conference on Experimental Safety Vehicles, Paris, France.

Kroell, C., Schneider, D., Nahum, A. (1971) Impact tolerance and response of the human thorax. Paper number 710851, Society of Automotive Engineers, Warrendale, Pennsylvania.

Kroell, C., Schneider, D., Nahum, A. (1974) Impact tolerance and response of the human thorax II. Paper number 741187, Society of Automotive Engineers, Warrendale, Pennsylvania.

Lizee, E., Robin, S., Song, E., Bertholon, N., Le Coz, J.-Y., Besnault, B., and Lavaste, F. (1998) Development of a 3D finite element model of the human body. Proc 42nd Stapp Car Crash Conference, SAE 983152.

Lobdell, T., Kroell, C., Schneider, D., Hering, W., Nahum, A. (1973) Impact Response of the Human Thorax in Proceedings of the Symposium Human Impact Response Measurement and Simulation. Edited by King W and Mertz H. General Motors Research Laboratories, Warren Michigan. Plenum Press New York, London, 1973, pp 201-245.

Murakami, D, Kitagawa, Y, Kobayashi, S, Kent, R, Crandall, J. (2004) Development and validation of a finite element model of a vehicle occupant. Paper 2004-01-0325, Society of Automotive Engineers, Warrendale, PA.

Petit, P., Trosseille, X., Baudrit, P., Gopal, M. (2003) Finite element simulation study of a frontal driver airbag deployment for out-of-position simulations. Stapp Car Crash Journal 47:211-242.

Plank, G. R., Kleinberger, M., and Eppinger, R. H. (1989) Computed dynamic response of the human thorax from a finite element model. Twelfth International Conference on Experimental Safety Vehicles.

Plank, G. R., Kleinberger, M., and Eppinger, R. H. (1994) Finite element modeling and analysis of thorax/restraint system interaction. Fourteenth International Conference on Experimental Safety Vehicles.

Plank, G. R., Kleinberger, M., and Eppinger, R. H. (1998) Analytical investigation of driver thoracic response to out of position airbag deployment. Proc 42nd Stapp Car Crash Conference, SAE 983165.

Ruan, J., El-Jawahri, R., Chai, L., Barbat, S., Prasad, P. (2003) Prediction and analysis of human thoracic impact responses and injuries in cadaver impacts using a full human body finite element model. Stapp Car Crash Journal 47:299-322.

Shaw, C., Lessley, D., Crandall, J., Kent, R., Kitis, L. (2005) Elimination of thoracic muscle tensing effects from frontal crash dummies. Paper 2005-01-0307 Society of Automotive Engineers, Warrendale, PA.

Stokes I. A. F., and Laible J. P. (1990) Three-dimensional osseo-ligamentous model of the thorax representing initiation of scoliosis by asymmetric growth. *J. Biomechanics* 23(6), pp. 589-595.

Viano, D. C., (1987a) Evaluation of the benefit From energy absorbing material in side impact protection: Part I. Proc 31st Stapp Car Crash Conference, SAE 872212.

Viano, D. C., (1987b) Evaluation of the benefit From energy absorbing material in side impact protection: Part II. Proc 31st Stapp Car Crash Conference, SAE 872213.

Wang K. H.-C. and Yang K. H. (1998) The development of a finite element human thorax model. Advances in Bioengineering, ASME, BED-Vol. 39.

Yoganandan, N., Pintar, F., Gennarelli, T. (2004) Small female-specific biomechanical corridors in side impacts. Proc. IRCOBI.

APPENDIX – Example force-deflection cross-plots

Data from subject 173 with diagonal belt and distributed loading conditions are shown as typical examples of the change in chest depth that occurs with denuding and eviscerating (note that eviscerating includes a tissue change as well as the removal of pulmonary pressurization) as well as typical examples of the increased sensitivity to tissue condition associated with a loading condition that does not engage the shoulder.